

End-to-End Variational Bayesian Training of Tensorized Neural Networks with Automatic Rank Determination

Cole Hawkins, Zheng Zhang, *Member, IEEE*

Abstract—Low-rank tensor decomposition is one of the most effective approaches to reduce the memory and computing requirements of large-size neural networks, enabling their efficient deployment on various hardware platforms. While post-training tensor compression can greatly reduce the cost of inference, uncompressed training still consumes excessive hardware resources, run-time and energy. It is highly desirable to directly train a compact low-rank tensorized model from scratch with a low memory and computational cost. However, this is a very challenging task because it is hard to determine a proper tensor rank *a priori*, which controls the model complexity and compression ratio in the training process.

This paper presents a novel end-to-end framework for low-rank tensorized training of neural networks. We first develop a flexible Bayesian model that can handle various low-rank tensor formats (e.g., CP, Tucker, tensor train and tensor-train matrix) that compress neural network parameters in training. This model can automatically determine the tensor ranks inside a nonlinear forward model, which is beyond the capability of existing Bayesian tensor methods. We further develop a scalable stochastic variational inference solver to estimate the posterior density of large-scale problems in training. Our work provides the first general-purpose rank-adaptive framework for end-to-end tensorized training. Our numerical results on various neural network architectures show orders-of-magnitude parameter reduction and little accuracy loss (or even better accuracy) in the training process.

I. INTRODUCTION

Despite their success in many applications, deep neural networks are often over-parameterized, requiring extensive computing resources in their training and inference. For instance, the VGG-19 network requires 500M memory [1] for image recognition; the DLRM deep learning recommendation system [2] has over 540M parameters, and the practical model deployed by Facebook is even larger. It has become a common practice to reduce the size of neural networks before deploying them in various scenarios ranging from cloud services to embedded systems to mobile applications.

Motivated by real-time inference and hardware resource constraints [3], numerous techniques have been developed to build *compact* models [4], [5], [6] after training. Representative approaches include pruning [6], quantization [7], knowledge distillation [8], and low-rank factorization [9], [10], [11],

[12], [13]. Among these techniques, low-rank tensor compression [12], [13], [14], [15] has achieved possibly the most significant compression, leading to promising reduction of FLOPS and hardware cost [12], [16], [17]. The recent progress of hardware design and algorithm/hardware co-design [16], [17], [18], [19], [20] of tensor operations can further reduce the run-time and boost the energy efficiency of tensorized models on clusters, FPGA and ASIC chips.

Training is a much more challenging task than inference, consuming much more money, run-time, energy, and hardware resources. A recent study [21] found that training some common natural language processing models on the cloud could emit $5\times$ carbon dioxide compared with the lifetime emissions of the average American car. Meanwhile, the increasing concerns about data privacy have become a driving force of training on resource-constrained edge devices [22]. These high costs and hardware constraints associated with neural network training motivate us to ask the following question: “*Is it possible to train a compact neural network model from scratch?*” Essentially, the computing and hardware cost could be significantly reduced on various platforms if we can avoid the full-size uncompressed training.

In order to address this challenge, we investigate end-to-end tensorized training, aiming to train compact models with orders-of-magnitude fewer parameters directly from scratch. This is a non-trivial task. The training cost, model complexity and accuracy are controlled by tensor ranks, which are unknown *a priori*. Exactly determining a tensor rank is NP-hard even for the simplest tensor factorization problems [23]. Some recent low-rank tensorized training methods [24], [25], [26] fix the tensor ranks, which are hard to guess or select in practice. One often has to perform extensive combinatorial searches and many training runs until a good rank parameter is found.

A. Contributions

This paper proposes a novel framework for end-to-end tensorized training of neural networks. Our training method uses a Bayesian model to determine both tensor ranks and factors automatically. Leveraging the recent advances in approximate Bayesian inference [27], we develop a scalable stochastic variational inference solver to efficiently infer the unknown variables of realistic neural networks in a single training run. We apply our method to train several neural network models [14], [24], [25], [26], achieving up to hundreds of times

This work is supported by xxx.

Cole Hawkins is with Department of Mathematics, University of California, Santa Barbara, CA 93106. E-mail: colehawkins@math.ucsb.edu.

Zheng Zhang is with Department of Electrical and Computer Engineering, University of California, Santa Barbara, CA 93106. E-mail: zhengzhang@ece.ucsb.edu.

parameter reduction with similar or even better accuracy in a single training run.

Many advances in tensor-based modeling are problem-specific and focus on a single tensor format. In contrast our work includes all four low-rank tensor formats in common use (CP, Tucker, tensor-train, and tensor-train matrix) and provides a framework to make general advances in low-rank tensor-based modeling. This paper focuses on tensorized neural networks, but our method can easily be applied to other tensor problems (e.g., tensor completion, tensor regression and multi-task tensor learning).

To the best of our knowledge, our work is the first proposed end-to-end method that automatically determines the tensor rank in neural network training, and the first Bayesian tensor solver to support multiple low-rank tensor formats simultaneously in realistic large neural networks.

B. Related Work

This work is related to the following previous results.

Rank Determination for Linear Tensor Problems. While exact tensor rank determination is NP-hard [23], some approximate methods have been developed to estimate the tensor ranks in tensor factorization and completion. Optimization-based approaches employ a heuristic tensor nuclear norm as the surrogate of tensor rank [28], [29], [30], but they require expensive regularization on the unfolded tensor. A nice alternative solution is to use Bayesian inference to automatically estimate tensor ranks from observed data [31], [32], [33], [34], [35]. Current Bayesian tensor methods solve tensor factorization, completion and regression problems on small-scale data where the observed data is a linear function of the hidden tensor. These problems allow closed-form parameter updates in mean-field Bayesian inference [32], [33], [34], [35]. Sampling-based Bayesian methods (i.e. MCMC) require storing thousands of copies of the model, which is not feasible for large neural networks. Because the mean-field variational approach for linear tensor problems [32], [36] does not work for tensorized neural networks, this paper develops a scalable solver based on stochastic variational inference [27].

Tensorized Neural Networks. Most work uses tensor decomposition to compress pre-trained neural networks. Examples include employing CP and Tucker factorizations to compress convolutional layers [12], [13]. In these examples the convolutional filters are already in a tensor form. It has been a common practice to reshape the weights in a fully connected layer to a high-order tensor, then a tensor factorization can achieve much higher a compression ratio than a matrix factorization on convolution layers [13]. Some recent approaches train low-rank tensorized neural networks [24], [25], [26] by assuming a low-rank tensorization with a fixed rank. While it is possible to tune the tensor ranks in post-training tensor compression [12], [13] based on approximation errors, one has to use manual tuning or combinatorial search to determine tensor ranks in existing tensorized training methods [24], [25], [26].

II. PRELIMINARIES

A. Tensors and Tensor Decomposition

This paper uses lower-case letters (e.g., a) to denote scalars, bold lowercase letters (e.g., \mathbf{a}) to represent vectors, bold uppercase letters (e.g., \mathbf{A}) to represent matrices, and bold calligraphic letters (e.g., \mathcal{A}) to denote tensors. A tensor is a generalization of a matrix, or a multi-way data array. An order- d tensor is a d -way data array $\mathcal{A} \in \mathbb{R}^{I_1 \times I_2 \times \dots \times I_d}$, where I_n is the size of mode n . The (i_1, i_2, \dots, i_d) -th element of \mathcal{A} is denoted as $a_{i_1 i_2 \dots i_d}$. An order-3 tensor is shown in Fig. 1 (a).

Definition 1: The mode- n product of a tensor $\mathcal{A} \in \mathbb{R}^{I_1 \times \dots \times I_n \times \dots \times I_d}$ with a matrix $\mathbf{U} \in \mathbb{R}^{J \times I_n}$ is

$$\mathcal{B} = \mathcal{A} \times_n \mathbf{U} \iff b_{i_1 \dots i_{n-1} j i_{n+1} \dots i_d} = \sum_{i_n=1}^{I_n} a_{i_1 \dots i_d} u_{j i_n}. \quad (1)$$

The result is still a d -dimensional tensor \mathcal{B} , but the mode- n size becomes J . In the special case $J = 1$, the n -th mode diminishes and \mathcal{B} becomes an order- $d - 1$ tensor.

A tensor has massive entries if d is large. This causes a high cost in both computing and storage. Fortunately, many practical tensors have a low-rank structure, and this property can be exploited to reduce the cost dramatically.

Definition 2: A d -way tensor $\mathcal{A} \in \mathbb{R}^{I_1 \times \dots \times I_d}$ is rank-1 if it can be written as a single outer product of d vectors

$$\mathcal{A} = \mathbf{u}^{(1)} \circ \dots \circ \mathbf{u}^{(d)}, \text{ with } \mathbf{u}^{(n)} \in \mathbb{R}^{I_n} \text{ for } n = 1, \dots, d.$$

Equivalently, each element of \mathcal{A} can be written as

$$a_{i_1 i_2 \dots i_d} = \prod_{n=1}^d u_{i_n}^{(n)},$$

where $u_{i_n}^{(n)}$ is the i_n -th element of the vector $\mathbf{u}^{(n)}$.

A rank-1 tensor can be stored with only d vectors. Most tensors are not rank-1, but many can be well-approximated via tensor decomposition [37] if their ranks are low. In this paper we will use the following four tensor decomposition formats to reduce the parameters of neural networks.

Definition 3: The CP factorization [38], [39] expresses a d -way tensor \mathcal{A} as the sum of multiple rank-1 tensors:

$$\mathcal{A} = \sum_{j=1}^R \mathbf{u}_j^{(1)} \circ \mathbf{u}_j^{(2)} \circ \dots \circ \mathbf{u}_j^{(d)}. \quad (2)$$

Here \circ denotes an outer product operator. The minimal integer R that ensures the equality is called the **CP rank** of \mathcal{A} . To simplify notation we collect the rank-1 terms of the n -th mode into a factor matrix $\mathbf{U}^{(n)} \in \mathbb{R}^{I_n \times R}$ with

$$\mathbf{U}^{(n)}(:, j) = \mathbf{u}_j^{(n)}. \quad (3)$$

A CP factorization with rank R can be described with d factor matrices $\{\mathbf{U}^{(n)}\}_{n=1}^d$ using $R \sum_n I_n$ parameters.

Definition 4: The Tucker factorization [40] expresses a d -way tensor \mathcal{A} as a series of mode- n products:

$$\mathcal{A} = \mathcal{G} \times_1 \mathbf{U}^{(1)} \times_2 \dots \times_d \mathbf{U}^{(d)}. \quad (4)$$

Here $\mathcal{G} \in \mathbb{R}^{R_1 \times \dots \times R_d}$ is a small core tensor, and $\mathbf{U}^{(n)} \in \mathbb{R}^{I_n \times R_n}$ is a factor matrix for the n -th mode. The **Tucker**

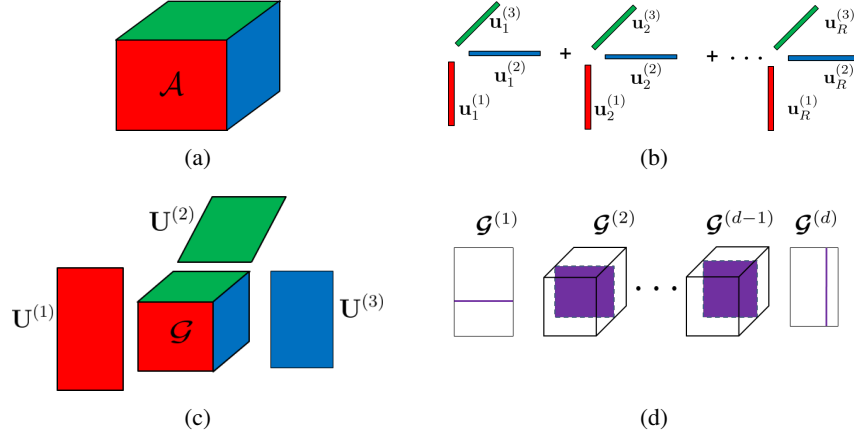


Fig. 1: (a): An order-3 tensor, (b) and (c): representations in CP and Tucker formats respectively, where low-rank factors are color-coded to indicate the corresponding modes. (d): TT representation of an order- d tensor, where the purple lines and squares indicate $\mathcal{G}^{(n)}(:, i_n, :)$, which is the i_n -th slice of the TT core $\mathcal{G}^{(n)}$ obtained by fixing its second index.

rank is the tuple (R_1, \dots, R_d) . A Tucker factorization with ranks $R_n = R$ requires $R^d + R \sum_n I_n$ parameters.

Definition 5: The tensor-train (TT) factorization [41] expresses a d -way tensor \mathcal{A} as a collection of matrix products:

$$a_{i_1 i_2 \dots i_d} = \mathcal{G}^{(1)}(:, i_1, :)\mathcal{G}^{(2)}(:, i_2, :)\dots\mathcal{G}^{(d)}(:, i_d, :). \quad (5)$$

Each TT-core $\mathcal{G}^{(n)} \in \mathbb{R}^{R_{n-1} \times I_n \times R_n}$ is an order-3 tensor. The tuple (R_0, R_1, \dots, R_d) is the **TT-rank** and $R_0 = R_d = 1$. The TT format uses $\sum_n R_{n-1} I_n R_n$ parameters in total and leads to more expressive interactions than the CP format.

Let $\mathbf{A} \in \mathbb{R}^{I \times J}$ be a matrix. We assume that the dimensions I and J can be factored as follows:

$$I = \prod_{n=1}^d I_n, J = \prod_{n=1}^d J_n. \quad (6)$$

We can reshape \mathbf{A} into a tensor \mathcal{A} with dimensions $I_1 \times \dots \times I_d \times J_1 \times \dots \times J_d$, such that the (i, j) -th element of \mathbf{A} uniquely corresponds to the $(i_1, i_2, \dots, i_d, j_1, j_2, \dots, j_d)$ -th element of \mathcal{A} . The TT decomposition can be extended to compress the resulting order- $2d$ tensor as follows.

Definition 6: The tensor-train matrix (TTM) factorization expresses an order- $2d$ tensor \mathcal{A} as d matrix products:

$$a_{i_1 \dots i_d j_1 \dots j_d} = \mathcal{G}^{(1)}(:, i_1, j_1, :)\mathcal{G}^{(2)}(:, i_2, j_2, :)\dots\mathcal{G}^{(d)}(:, i_d, j_d, :). \quad (7)$$

Here each TT-core $\mathcal{G}^{(n)} \in \mathbb{R}^{R_{n-1} \times I_n \times J_n \times R_n}$ is an order-4 tensor. The tuple $(R_0, R_1, R_2, \dots, R_d)$ is the **TT-rank** and as before $R_0 = R_d = 1$. This TTM factorization requires $\sum_n R_{n-1} I_n J_n R_n$ parameters to represent \mathcal{A} .

We provide a visual representation of the CP, Tucker, and TT formats in Fig. 1 (b) – (d).

B. Deep Neural Networks

A deep neural network can be written as

$$\mathbf{y} = \mathbf{h}(\mathbf{x}) = \mathbf{g}_L(\mathbf{g}_{L-1}(\dots \mathbf{g}_1(\mathbf{x}))) \quad (8)$$

where $\mathbf{g}_k(\circ)$ represents layer k , \mathbf{x} is an input data sample (e.g., an image) and \mathbf{y} is a predicted output label. In this work we focus on the following types of layers:

- **Fully connected layer:** A fully-connected layer \mathbf{g}_k is

$$\mathbf{g}_k(\mathbf{x}_k) = \sigma(\mathbf{W}_k \mathbf{x}_k + \mathbf{b}_k) \quad (9)$$

where σ is a nonlinear activation function (e.g., ReLU or sigmoid function), \mathbf{W}_k is a weight matrix, and \mathbf{b}_k is a bias vector. Most parameters in a fully connected layer are contained in the weight matrix \mathbf{W}_k .

- **Embedding layer:** An embedding layer is defined as

$$\mathbf{g}_k(\mathbf{X}_k) = \mathbf{W}_k \mathbf{X}_k \quad (10)$$

where \mathbf{W}_k is the embedding matrix and the \mathbf{X}_k is a sparse matrix with entries restricted to $\{0, 1\}$. This type of layer is a common first layer of deep neural networks employed in natural language processing and recommendation tasks [26].

- **Convolutional layer:** A convolutional layer is

$$\mathbf{g}_k(\mathcal{X}_k) = \sigma(\mathcal{W}_k \star \mathcal{X}_k + \mathbf{b}_k) \quad (11)$$

where σ is a nonlinear activation function, \mathcal{W}_k is a weight tensor, \mathcal{X}_k is the input tensor of layer k , “ \star ” is a convolution operator, and \mathbf{b}_k is a bias. For instance, let $\mathcal{W} \in \mathbb{R}^{l \times l \times C_{\text{in}} \times C_{\text{out}}}$ be a 2D convolution for image processing with filter size $l \times l$, C_{in} input channels, and C_{out} output channels. The convolution operation is defined as

$$\mathcal{Y} = \mathcal{W} \star \mathcal{A} \iff y_{xyz} = \sum_{i=1}^l \sum_{j=1}^l \sum_{c=1}^{C_{\text{in}}} w_{ijcz} a_{x+i-1, y+j-1, c}. \quad (12)$$

Considering parameter dependence, we can re-write (8) as

$$\mathbf{y} = \mathbf{h}(\mathbf{x} \mid \{\mathbf{W}_k, \mathbf{b}_k\}_{k=1}^L). \quad (13)$$

In a convolution layer \mathbf{W}_k should be replaced with \mathcal{W}_k .

C. Tensorized Neural Networks

In a modern neural network, $\{\mathbf{W}_k\}_{k=1}^L$ contain millions to billions of parameters. The resulting model consumes a huge amount of memory, energy and run-time in training and inference. This has become a major challenge across various hardware platforms. A promising solution is to generate a compact neural network via low-rank tensor compression [13], [14], [24] as follows:

- **Folding to high-order tensors.** A general weight matrix $\mathbf{W} \in \mathbb{R}^{I \times J}$ can fold into an order- d tensor $\mathcal{A} \in \mathbb{R}^{I_1 \times \dots \times I_d}$ where $IJ = \prod_n I_n$. We can also fold \mathbf{W} to an order- $2d$ tensor $\mathcal{A} \in \mathbb{R}^{I_1 \times \dots \times I_d \times J_1 \times \dots \times J_d}$ such that $w_{ij} = a_{i_1 \dots i_d j_1 \dots j_d}$. While a convolution filter is already a tensor, we can reshape it to a higher-order tensor with reduced mode sizes.
- **Low-rank tensor compression.** After folding a weight matrix or convolution filter into a higher-order tensor \mathcal{A} , one can employ low-rank tensor compression to reduce the number of parameters. Either the CP, Tucker, TT or TTM factorization can be applied [12], [13], [14], [14].

Assume that Φ_k includes all low-rank tensor factors required to represent \mathbf{W}_k . Considering the dependence of \mathbf{W}_k on Φ_k , we can now write (13) as

$$\begin{aligned} \mathbf{y} &= \mathbf{h}(\mathbf{x} \mid \{\mathbf{W}_k(\Phi_k), \mathbf{b}_k\}_{k=1}^L) \\ &= \mathbf{f}(\mathbf{x} \mid \Psi), \text{ with } \Psi = \{\Phi_k, \mathbf{b}_k\}_{k=1}^L. \end{aligned} \quad (14)$$

Please note the following:

- The tensor factors in Φ_k depend on the tensor format we choose. For instance, in CP format, Φ_k only includes d matrix factors; in a Tucker format, Φ_k includes d factor matrices and a small-size order- d core tensor as shown in (4); when the TT or TTM format is used, Φ_k includes d order-3 or order-4 TT cores shown in (5) and (7) respectively. Different tensor formats can lead to different compression ratios.
- The number of variables in each Φ_k depends on the tensor ranks used in the compression. A higher tensor rank leads to higher expressive power but a lower compression ratio. In existing approaches, it is hard to select a proper tensor rank *a-priori*. We hope to address this issue in this paper.
- Ψ include all tensor factors and bias vectors of all layers in a tensorized neural network. The variables in Ψ is often orders-of-magnitude fewer than that in the original model (13).
- The function \mathbf{f} has included the process of mapping Φ_k back to its associated weight matrix \mathbf{W}_k in addition to the forward evaluation of function \mathbf{h} .

Two current approaches exist to produce low-rank, tensor-compressed neural networks. The first is the train-then-compress approach which trains an uncompressed neural network \mathbf{h} and then performs tensor factorization on each of the weights $\{\mathbf{W}_k\}_{k=1}^L$. The train-then-compress approach suffers from two drawbacks.

- **High training costs.** The network \mathbf{h} is trained in uncompressed format so the training device must support the

memory, compute, and energy requirements of a huge-size network.

- **Lower accuracy.** After the initial training, the weights $\{\mathbf{W}_k\}_{k=1}^L$ must be decomposed to low-rank tensor format [12], [13]. The tensor factorization followed by fine-tuning may greatly reduce model accuracy, especially when the weights produced by uncompressed training possess no hidden low-rank structure.

The second approach is fixed-rank tensorized training. In this approach the user pre-specifies the tensor rank and trains low-rank tensor factors of weight parameters. This approach avoids the compute and memory requirements of uncompressed training but requires that the user manually select a good rank *a-priori*. This approach usually requires multiple training runs to select the rank. In addition a user-specified rank may achieve suboptimal compression.

III. BAYESIAN LOW-RANK TENSORIZED MODEL

In this work, we plan to develop a tensorized training method that can automatically determine the tensor ranks in the training process. This method requires only one run of training and avoids the high cost of uncompressed training.

It is hard to determine tensor ranks in the training process. Exactly determining the tensor rank is NP-hard [23], [37]. Unlike matrix factorization which often uses the nuclear norm as a convex surrogate of matrix rank [42], there are no rigorous surrogate models for tensor ranks. Existing heuristic surrogates [28], [29], [30] only work for small-size tensors due to the memory-consuming tensor unfolding operations. In this paper we will develop a Bayesian approach for rank determination in tensorized neural networks. Bayesian methods have been employed for tensor completion and factorization [32], [33], [36], where the observed data is a linear function of tensor elements. However, existing Bayesian tensor solvers do not work for tensorized neural networks due to the nonlinear forward model and large number of unknown variables.

A. High-Level Bayesian Formulation

We first describe a general-purpose Bayesian model for training low-rank tensorized neural networks. For notational convenience we assume that our neural network model \mathbf{f} has one nonlinear layer, and that its weight matrix \mathbf{W} is folded to a single tensor \mathcal{A} . Extending our method to general multi-layer cases with multiple tensors is straightforward, and we will report numerical results on general multi-layer models in Section V.

Given a training data set \mathcal{D} , our goal is determine the unknown low-rank factors Φ for \mathcal{A} , the associated tensor ranks and bias vector \mathbf{b} . We introduce some hyper parameters Λ to control the tensor ranks and model complexity in our Bayesian model. Our posterior distribution is

$$p(\Psi, \Lambda \mid \mathcal{D}) = \frac{p(\mathcal{D} \mid \Psi)p(\Psi, \Lambda)}{p(\mathcal{D})}, \text{ with } \Psi = \{\Phi, \mathbf{b}\}. \quad (15)$$

Here $p(\mathcal{D} \mid \Psi)$ is the model likelihood, $p(\Psi, \Lambda)$ is the joint prior and $p(\mathcal{D})$ is the model evidence defined by

$$p(\mathcal{D}) = \int_{\Psi, \Lambda} p(\mathcal{D} \mid \Psi)p(\Psi, \Lambda)d\Psi d\Lambda. \quad (16)$$

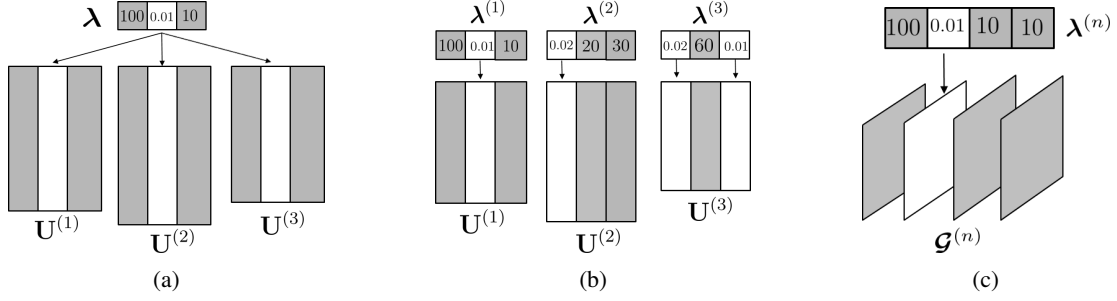


Fig. 2: (a) For the CP prior, if one element of λ is small, one column is removed from every factor matrix. (b) For the Tucker prior, if one element of $\lambda^{(n)}$ is small then one column of $\mathbf{U}^{(n)}$ shrinks to zero. (c) For the TT prior, if one element of $\lambda^{(n)}$ is small then one slice of $\mathcal{G}^{(n)}$ shrinks to zero. The columns/slices to be removed are marked in white.

The likelihood and joint prior are specified below:

- **Likelihood function:** $p(\mathcal{D}|\Psi)$ and data \mathcal{D} are determined by a forward propagation model. Our proposed method is suitable for any differentiable likelihood function. In this work we focus on neural network classification problems with a multinomial likelihood function. Let $(\mathbf{x}, \mathbf{y}) \in \mathcal{D}$ be a training sample where \mathbf{x} is the neural network input and \mathbf{y} is the associated true label. The likelihood is

$$p(\mathcal{D}|\Psi) = \prod_{(\mathbf{x}, \mathbf{y}) \in \mathcal{D}} \text{Mult}(\mathbf{y}|\mathbf{f}(\mathbf{x}|\Psi)). \quad (17)$$

Here Mult is the multinomial distribution probability density function, and \mathbf{f} is the forward propagation model as specified in (14) which is conditioned on the given low-rank tensor factors and bias vectors.

- **Joint Prior:** We place an independent prior over the low-rank tensor factors and the bias term. We also choose a weak normal prior for the bias term:

$$p(\Psi, \Lambda) = p(\mathbf{b})p(\Phi, \Lambda), \quad (18)$$

$$p(\mathbf{b}) = \prod_i \mathcal{N}(b_i|0, \sigma_0^2).$$

Here $p(\Phi, \Lambda)$ is the joint prior for the low-rank tensor factors Φ and the rank-controlling hyper parameter Λ . The design of $p(\Phi, \Lambda)$ is non-trivial and depends on the tensor format we choose for the model, which will be explained in Section III-B & III-C.

B. Tensor Factor Priors

Proper priors should be chosen for the tensor factors in order to automatically enforce low-rank compression in the training process. The low-rank tensor factors in Φ and their influence on the forward model \mathbf{h} depends on the tensor format we choose. Therefore, we will specify the joint prior $p(\Phi, \Lambda)$ for the four tensor formats described in Section II-A: CP, Tucker, TT and TTM.

Firstly we specify the general form of $p(\Phi, \Lambda)$.

- For the CP format, we initialize each factor $\mathbf{U}^{(n)}$ as a matrix with R columns. Assume that R is larger than the actual rank r , and all factors shrink to r columns in the training process. Because all factors have the same maximum rank (number of columns), we use a single vector $\Lambda = \lambda \in \mathbb{R}^R$ to control the rank.

- In contrast, the tensor ranks of Tucker, TT and TTM formats are a vector, and the rank associated with each mode can be different. Therefore, for an order- d tensor, we need a collection of vectors $\Lambda = \{\lambda^{(n)}\}_{n=1}^d$ to control the ranks of each mode individually. Here $\lambda^{(n)} \in \mathbb{R}^{R_n}$, and the “maximum rank” R_n is above r_n (the actual rank of mode n).

As a result, we introduce the general form

$$p(\Phi, \Lambda) = \begin{cases} p(\Phi|\lambda)p(\lambda) & \text{for CP format} \\ p(\Phi|\{\lambda^{(n)}\}) \prod_{n=1}^d p(\lambda^{(n)}) & \text{for Tucker, TT \& TTM} \end{cases} \quad (19)$$

where the prior distribution(s) on λ or $\{\lambda^{(n)}\}_{n=1}^d$ enforce rank reduction.

Next we specify the tensor factor priors $p(\Phi|\lambda)$ or $p(\Phi|\{\lambda^{(n)}\})$ for each tensor format, and we defer the prior of λ and $\{\lambda^{(n)}\}_{n=1}^d$ to Section III-C.

- **CP Format:** The tensor factors in a CP factorization are d matrices, therefore $\Phi = \{\mathbf{U}^{(n)}\}_{n=1}^d$. We assign a Gaussian prior with controllable variance to each element of each factor matrix $\mathbf{U}^{(n)}$:

$$p(\Phi, \Lambda) = p(\lambda) \prod_n p(\mathbf{U}^{(n)}|\lambda), \quad (22)$$

$$p(\mathbf{U}^{(n)}|\lambda) = \prod_{i,j} \mathcal{N}(u_{ij}^{(n)}|0, \lambda_j).$$

Here $u_{ij}^{(n)}$ is the (i, j) -th element of $\mathbf{U}^{(n)}$. Each entry of λ controls one column of each factor matrix. If a single entry λ_j approaches zero, then the prior mean and prior variance of $u_{ij}^{(n)}$ are both close to zero for all row indices $i \in [1, I_n]$ and mode indices $n \in [1, d]$. This encourages the whole j -th column of $\mathbf{U}^{(n)}$ to shrink to zero, leading to a rank reduction. The vector λ is shared across all modes, therefore it will shrink the same column of all CP factor matrices $\{\mathbf{U}^{(n)}\}_{n=1}^d$ simultaneously, as shown in Fig. 2 (a).

- **Tucker Format:** A Tucker factorization includes a core tensor and d factor matrices, therefore $\Phi = \{\mathcal{G}, \{\mathbf{U}^{(n)}\}_{n=1}^d\}$. Similar to the CP model, each factor matrix $\mathbf{U}^{(n)}$ is assigned a Gaussian distribution with controllable variances. Unlike the CP model, a Tucker model has d separate rank parameters (r_1, \dots, r_d) to

$$p(\Phi, \Lambda) = p(\mathcal{G}^{(d)} | \lambda^{(d-1)}) \prod_{1 \leq n \leq d-1} p(\mathcal{G}^{(n)} | \lambda^{(n)}) p(\lambda^{(n)}),$$

$$p(\mathcal{G}^{(n)} | \lambda^{(n)}) = \prod_{i,j,k} \mathcal{N}(g_{ijk}^{(n)} | 0, \lambda_k^{(n)}) \text{ for } n \in [1, d-1], \text{ and } p(\mathcal{G}^{(d)} | \lambda^{(d-1)}) = \prod_{i,j,k} \mathcal{N}(g_{ijk}^{(d)} | 0, \lambda_i^{(d-1)}). \quad (20)$$

$$p(\Phi, \Lambda) = p(\mathcal{G}^{(d)} | \lambda^{(d-1)}) \prod_{1 \leq n \leq d-1} p(\mathcal{G}^{(n)} | \lambda^{(n)}) p(\lambda^{(n)}),$$

$$p(\mathcal{G}^{(n)} | \lambda^{(n)}) = \prod_{i,j,k,l} \mathcal{N}(g_{ijkl}^{(n)} | 0, \lambda_l^{(n)}), \text{ for } n \in [1, d-1], \text{ and } p(\mathcal{G}^{(d)} | \lambda^{(d-1)}) = \prod_{i,j,k,l} \mathcal{N}(g_{ijkl}^{(d)} | 0, \lambda_i^{(d-1)}). \quad (21)$$

determine, one per factor matrix as shown in Fig. 2 (b). Furthermore, the factor matrices and core tensor are handled separately. Therefore, we propose the following prior distributions:

$$p(\Phi, \Lambda) = p(\mathcal{G}) \prod_n p(\mathbf{U}^{(n)} | \lambda^{(n)}) p(\lambda^{(n)}),$$

$$p(\mathbf{U}^{(n)} | \lambda^{(n)}) = \prod_{i,j} \mathcal{N}(u_{ij}^{(n)} | 0, \lambda_j^{(n)}).$$

We use d independent rank controlling vectors $\{\lambda^{(n)}\}_{n=1}^d$ to control the prior variances of different factor matrices separately. The j -th element of $\lambda^{(n)}$ controls the j -th column of factor matrix $\mathbf{U}^{(n)}$. Therefore $\lambda^{(n)}$ controls r_n , the n -th entry of the Tucker rank. We place a weak normal prior over the entries of the core tensor \mathcal{G} :

$$p(\mathcal{G}) = \prod_{i_1, \dots, i_d} \mathcal{N}(g_{i_1 \dots i_d} | 0, \sigma_0^2). \quad (23)$$

We make this choice to simplify parameter inference compared to the alternative of placing low-rank priors on both of the core tensor and the factor matrices.

- **Tensor-Train (TT) Format:** A TT factorization uses d order-3 TT cores to represent an order- d tensor, therefore $\Phi = \{\mathcal{G}^{(n)}\}_{n=1}^d$. The TT format requires a more complicated prior because each low-rank factor $\mathcal{G}^{(n)} \in \mathbb{R}^{r_{n-1} \times I_n \times r_n}$ depends on two rank parameters r_{n-1} and r_n . In order to automatically determine the TT rank, we choose $R_n > r_n$, and initialize the n -th TT core with size $R_{n-1} \times I_n \times R_n$. The prior density of all TT cores are given in Eq. (20). We introduce a vector $\lambda^{(n)} \in \mathbb{R}^{R_n}$ to directly control the actual rank r_n for mode 1 to $d-1$. As shown in Fig. 2 (c), the k -th element of $\lambda^{(n)}$ (i.e., $\lambda_k^{(n)}$) controls the prior variance of a slice $\mathcal{G}^{(n)}(:, :, k)$. If $\lambda_k^{(n)}$ is small, then a whole slice of $\mathcal{G}^{(n)}$ is close to zero, leading to a rank reduction in the n -th mode. The only rank parameter that controls two separate cores is $\lambda^{(d-1)}$. This prevents any rank parameters from overlapping and it simplifies posterior inference.
- **Tensor-Train Matrix (TTM) Format:** Similar to the TT format, a TTM decomposition also has d core tensors, therefore $\Phi = \{\mathcal{G}^{(n)}\}_{n=1}^d$. The only difference is that each $\mathcal{G}^{(n)}$ is an order-4 tensor, which is initialized with a size $R_{n-1} \times I_n \times J_n \times R_n$ in our Bayesian model.

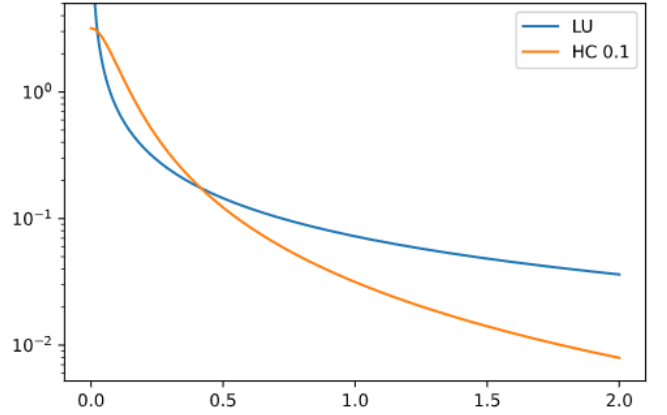


Fig. 3: Comparison of the probability density functions of the Log-Uniform and Half-Cauchy ($\eta = 0.1$) distributions.

The prior for the TTM low-rank factors is shown in (21), which is very similar to that of TT format. We use a vector parameter $\lambda^{(n)}$ to control the actual rank r_n of the n -th mode for $n \in [1, d-1]$, and $\lambda^{(d-1)}$ is shared among $\mathcal{G}^{(d)}$ and $\mathcal{G}^{(d-1)}$.

C. Rank-Shrinking Hyper-Parameter Priors

To complete the setup of Bayesian model (15), we still need to specify the prior of rank-control hyper parameters $\Lambda = \lambda$ (for CP) or $\Lambda = \{\lambda^{(n)}\}_{n=1}^d$ (for Tucker, TT and TTM). Note that small elements in λ and $\lambda^{(n)}$ leads to rank reductions in the tensor models, therefore we choose two hyper-prior densities that place high probability near zero. We focus our notation in this subsection on the CP model for simplicity.

We consider two choices of prior on the hyper parameter λ : the Half-Cauchy and improper Log-Uniform on $(0, \infty)$:

$$p(\lambda) = \prod_{i=1}^R p(\lambda_i), \quad \text{with } p(\lambda_i) = \begin{cases} \text{HC}(\lambda_i | 0, \eta) & \text{or} \\ \text{LU}(\lambda_i) & \end{cases} \quad (24)$$

The improper Log-uniform distribution has a fatter tail than the Half-Cauchy distribution and is parameter-free. We illustrate the probability density functions of both densities in Fig. 3. The Half-Cauchy scaling parameter η offers the advantage that the user can adjust η to tune the tradeoff

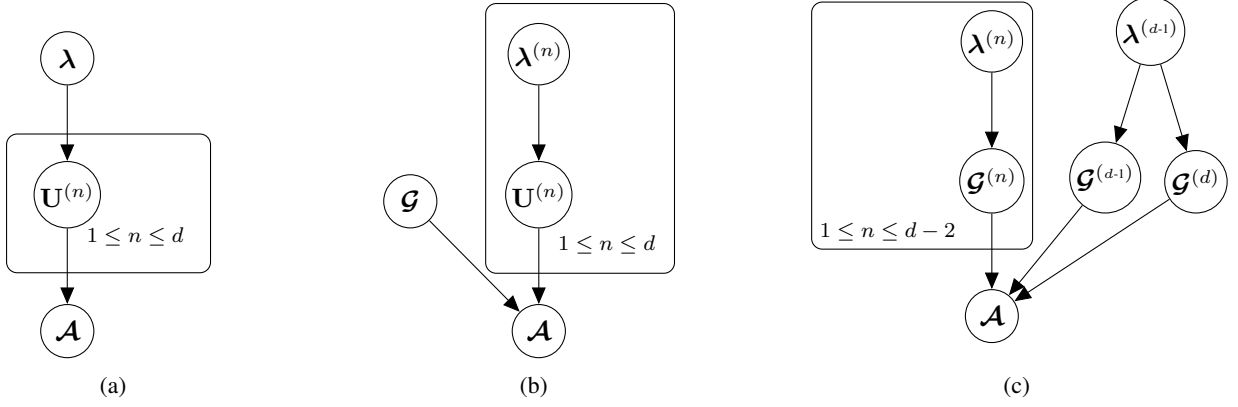


Fig. 4: (a) CP graphical model (b) Tucker graphical model (c) TT/TTM graphical model.

between accuracy and rank-sparsity but requires additional tuning. Both the Half-Cauchy density function

$$\text{HC}(\lambda_i|0, \eta) \propto \frac{1}{1 + \frac{\lambda_i^2}{\eta^2}} \quad (25)$$

and the Log-Uniform density function

$$\text{LU}(\lambda_i) \propto \frac{1}{\lambda_i} \quad (26)$$

place high probability in regions where λ_i is close to zero. The parameter λ controls the prior variance of the tensor factors in Φ , all of which have prior mean zero. Therefore the prior density encodes a prior belief that the tensor rank is low. Since each element of λ controls an entire column of every tensor factor, the prior density encourages structured rank shrinkage. We provide a visual description of our low-rank tensor prior in addition to Bayesian graphical models for each low-rank tensor format in Fig. 4.

IV. PARAMETER INFERENCE

Next we discuss how to estimate the resulting posterior density (15). We develop an approach based on stochastic variational inference (SVI) [27] that is compatible with the large-scale stochastic optimization required to train large neural networks. We employ SVI as our probabilistic inference method due to its computational efficiency and memory efficiency. Alternative inference methods such as MCMC [43], [44] and Stein variational gradient descent [45] require storing multiple copies of the entire neural network for both training and inference. This increases both memory and compute requirements by orders of magnitude [44] and is unsuitable for application scenarios with constrained computing resources. The mean-field variational inference in [32], [36] does not require storing multiple copies of model parameters, but its closed-form updates in the expectation-maximization steps only work for simple problems such as tensor completion and factorization.

In this section, we firstly describe the SVI method [27] for general Bayesian inference. Next, we highlight some obstacles to a straightforward implementation in our problem setting. Then we select a suitable approximate posterior to model the true posterior induced by our low-rank tensor prior. Finally,

we present an efficient inference method designed for our tensorized training with rank determination.

A. Stochastic Variational Inference

Stochastic variational inference (SVI) [27] is a popular method for scalable Bayesian machine learning. Let θ be the parameters to infer and let $q(\theta)$ be the approximating distribution to the target posterior distribution

$$p(\theta|\mathcal{D}) \propto p(\mathcal{D}|\theta)p(\theta).$$

SVI is formulated as an optimization problem where the loss function is the KL divergence and the goal is to find the best approximating density q^* among a parameterized class of densities \mathcal{P} :

$$q^*(\theta) = \arg \min_{q(\theta) \in \mathcal{P}} \text{KL}(q(\theta)||p(\theta|\mathcal{D})) \quad (27)$$

$$\text{KL}(q(\theta)||p(\theta|\mathcal{D})) = \mathbb{E}_{q(\theta)} \left[\log \frac{q(\theta)}{p(\theta|\mathcal{D})} \right].$$

We rearrange the KL divergence to illustrate the requirements on the approximating distribution q :

$$\begin{aligned} \text{KL}(q(\theta)||p(\theta|\mathcal{D})) &= \mathbb{E}_{q(\theta)} [\log q(\theta) - \log p(\mathcal{D}|\theta) - \log p(\theta)] + \text{const.} \\ &= -\mathbb{E}_{q(\theta)} [\log p(\mathcal{D}|\theta)] + \text{KL}(q(\theta)||p(\theta)) + \text{const.} \end{aligned} \quad (28)$$

The first line follows from the Bayes rule and the second from the definition of the KL divergence. Therefore the objective function is a combination of the log-likelihood (model fit) and the divergence from the approximate posterior to the prior (low-rank). To approximate the log-likelihood one samples from the variational distribution q . The KL-divergence is either approximated via sampling or evaluated in a closed form depending on the model specification. The form in Equation (28) requires the evaluation of the full-data model likelihood. If the data is large the full-data likelihood $p(\mathcal{D}|\theta)$ is intractable, so we approximate the likelihood by subsampling a minibatch $\mathcal{M} \subset \mathcal{D}$.

B. Challenges of Nonlinear Rank Determination

We aim to construct a variational posterior $q(\theta)$ that is well-suited to the rank determination of tensorized neural networks, which is beyond the capability of existing Bayesian tensor factorization/completion solvers [31], [32], [36].

We focus our notation on the CP model parameters

$$\theta = \{\Phi, \Lambda\} = \{\{\mathbf{U}^{(n)}\}_{n=1}^d, \lambda\} \quad (29)$$

for clarity. The extension to the other three tensor models and to multi-layer networks is straightforward. We ignore the bias term \mathbf{b} which is assigned a factored normal variational posterior and follows well-studied update rules [46]. We use the mean-field approximation [47] for tractable optimization:

$$q(\{\mathbf{U}^{(n)}\}, \lambda) = q(\{\mathbf{U}^{(n)}\})q(\lambda). \quad (30)$$

We further model the posterior of tensor factors with a normal distribution

$$q(\{\mathbf{U}^{(n)}\}) = \prod_{n=1}^d q(\mathbf{U}^{(n)}), \quad (31)$$

$$q(\mathbf{U}^{(n)}) = \prod_{i,j} \mathcal{N}(u_{ij}^{(n)} | \overline{u_{ij}^{(n)}} , \Sigma_{ij}^{(n)2}),$$

where $\overline{u_{ij}^{(n)}}$ and $\Sigma_{ij}^{(n)}$ are the (i, j) -th elements of the unknown posterior mean $\overline{\mathbf{U}^{(n)}}$ and posterior standard deviation $\Sigma^{(n)}$ to be inferred, respectively.

Now we discuss the challenges in learning the variational posterior distribution. We modify Eq. (28) to obtain our objective function:

$$\begin{aligned} \mathcal{L}(q) = & -\mathbb{E}_{q(\{\mathbf{U}^{(n)}\}, \lambda)} \log p(\mathcal{D} | \{\mathbf{U}^{(n)}\}) \\ & + \text{KL} \left(q(\{\mathbf{U}^{(n)}\}, \lambda) \parallel p(\{\mathbf{U}^{(n)}\}, \lambda) \right) \end{aligned} \quad (32)$$

Two coupled challenges prevent us from applying the techniques of [31], [32], [36] in minimizing $\mathcal{L}(q)$:

- Firstly, the nonlinear forward model of a neural network requires gradient-based optimizations. In tensor completion the popular mean-field inference approach cycles through closed-form updates to select the optimal tensor factor parameters [32], [36]. In our problem of tensorized neural networks, no closed-form updates exist to select the optimal parameters. To optimize the tensor factors we must sample $\{\mathbf{U}^{(n)}\}$ from q and update the factors based on the gradient of the objective function.
- Secondly, a naive rank shrinkage may lead to high-variance gradients of the KL-divergence term. To demonstrate this issue we examine the gradients with respect to the parameters $\overline{u_{ij}^{(n)}}$ and $\Sigma_{ij}^{(n)}$. To sample the factor matrix entries we apply the re-parameterization trick [48]:

$$u_{ij}^{(n)} = \overline{u_{ij}^{(n)}} + z \Sigma_{ij}^{(n)}, \quad z \sim \mathcal{N}(0, 1). \quad (33)$$

The KL divergence satisfies the proportionality relation

$$\text{KL} \left(\mathcal{N}(\overline{u_{ij}^{(n)}} , \Sigma_{ij}^{(n)2}) \parallel \mathcal{N}(0, \lambda_j) \right) \propto \frac{\overline{u_{ij}^{(n)}}^2 + \Sigma_{ij}^{(n)2}}{\lambda_j} \quad (34)$$

which poses a challenge as λ_j approaches 0 due to rank shrinkage. Let $\phi \in \{\overline{u_{ij}^{(n)}} , \Sigma_{ij}^{(n)}\}$ represent either parameter of the posterior distribution of $u_{ij}^{(n)}$. If we sample $\lambda_j \sim q(\lambda_j)$ then the gradient variance conditioned on $u_{ij}^{(n)}$ is

$$\mathbb{V} \left[\nabla_{\phi} \text{KL} \left(\mathcal{N}(\overline{u_{ij}^{(n)}} , \Sigma_{ij}^{(n)2}) \parallel \mathcal{N}(0, \lambda_j) \right) \mid u_{ij}^{(n)} \right] \propto \mathbb{V} \left[\frac{1}{\lambda_j^2} \right]. \quad (35)$$

The goal of our low-rank prior is to shrink many $\lambda_j \rightarrow 0$. Therefore the values of $\frac{1}{\lambda_j^2}$ may be extremely large. If the distribution of λ_j is non-degenerate, as the posterior probability of λ_j concentrates around 0 even small uncertainties of λ_j will lead to large variance in Equation (35). This implies that a rank shrinkage can cause high-variance gradients which in turn may increase the magnitude of factor matrix parameters. Therefore a sampling-based gradient estimation of the KL divergence for nonlinear rank determination is not a viable option.

One alternative to the sampling-based gradient estimation is to seek a distribution $q(\lambda_k)$ that leads to a closed-form expression for the KL divergence. However known distributions that permit a closed-form KL divergence require a hierarchical Bayesian parameterization of the rank parameter λ [49], [50]. Such hierarchical Bayesian parameterizations require up to five additional hyperparameters for the new random variables in the parametrization [49]. Additional hyperparameters would require additional tuning runs during tensorized training so we disregard this option.

C. Variational Inference for Hyper Parameters

To avoid the above challenges we propose a deterministic approximation to the rank-controlling hyper parameter λ :

$$q(\lambda) = \delta_{\bar{\lambda}}(\lambda) \quad (36)$$

where $\bar{\lambda}$ is the posterior mean of λ . This delta approximation was used for probabilistic tensor factorization in [51]. This approximation admits closed-form updates to the following sub-problem when the factor matrices are fixed:

$$\arg \min_{\bar{\lambda}_k} \text{KL} \left(q(\{\mathbf{U}^{(n)}\}, \lambda) \parallel p(\{\mathbf{U}^{(n)}\}, \lambda) \right). \quad (37)$$

To obtain the update for $\bar{\lambda}_k$ we evaluate the KL divergence from the variational distribution to the prior, set the derivative with respect to $\bar{\lambda}_k$ equal to zero, and solve for $\bar{\lambda}_k$. We derive the closed-form updates to a single rank parameter $\bar{\lambda}_k$ for the CP model. Other models are similar. In Equation (38) we rearrange the KL divergence to the prior to isolate all terms involving the rank parameter $\bar{\lambda}_k$. Taking the derivative of the expression in Equation (39) with a Log-Uniform rank prior $p(\bar{\lambda}_k)$ yields

$$\begin{aligned} & \frac{\partial}{\partial \bar{\lambda}_k} \text{KL} \left(q(\{\mathbf{U}^{(n)}\}, \lambda) \parallel p(\{\mathbf{U}^{(n)}\}, \lambda) \right) \\ & \propto \sum_{1 \leq n \leq d} \sum_{1 \leq i \leq I_n} \left(\frac{1}{2\bar{\lambda}_k} - \frac{\overline{u_{ik}^{(n)}}^2 + \Sigma_{ik}^{(n)2}}{2\bar{\lambda}_k^2} \right) + \frac{1}{\bar{\lambda}_k}. \end{aligned} \quad (39)$$

$$\begin{aligned}
\text{KL}\left(q\left(\{\mathbf{U}^{(n)}\}, \boldsymbol{\lambda}\right) \| p\left(\{\mathbf{U}^{(n)}\}, \boldsymbol{\lambda}\right)\right) &= \text{KL}\left(q\left(\{\mathbf{U}^{(n)}\}\right) \| p\left(\{\mathbf{U}^{(n)}\} | \boldsymbol{\lambda}\right)\right) + \text{KL}\left(q(\boldsymbol{\lambda}) \| p(\boldsymbol{\lambda})\right) \\
&= \sum_{1 \leq n \leq d} \sum_{1 \leq i \leq I_n, 1 \leq j \leq R} \text{KL}\left(\mathcal{N}\left(\overline{u_{ij}^{(n)}}, \Sigma_{ij}^{(n)2}\right) \| \mathcal{N}(0, \lambda_j)\right) + \sum_{1 \leq j \leq R} \text{KL}\left(\delta(\lambda_j) \| p(\lambda_j)\right) \\
&\propto \sum_{1 \leq n \leq d} \sum_{1 \leq i \leq I_n} \text{KL}\left(\mathcal{N}\left(\overline{u_{ik}^{(n)}}, \Sigma_{ik}^{(n)2}\right) \| \mathcal{N}(0, \lambda_k)\right) - p(\lambda_k) \\
&\propto \sum_{1 \leq n \leq d} \sum_{1 \leq i \leq I_n} \left(\log \sqrt{\lambda_k} + \frac{\overline{u_{ik}^{(n)}}^2 + \Sigma_{ik}^{(n)2}}{2\lambda_k} \right) - p(\lambda_k)
\end{aligned} \tag{38}$$

We assign the notation

$$D = \sum_n I_n, \quad M = \sum_{1 \leq n \leq d} \sum_{1 \leq i \leq I_n} \overline{u_{ik}^{(n)}}^2 + \Sigma_{ik}^{(n)2}. \tag{40}$$

The number of entries controlled by λ_j is D , and M is their combined magnitude and variance. Enforcing (39) to be zero yields a closed-form update for the log-uniform prior:

$$\bar{\lambda}_k^* \leftarrow \frac{M}{D+1}. \tag{41}$$

In the case of the Half-Cauchy prior the update is

$$\bar{\lambda}_k^* \leftarrow \frac{M - \eta^2 D + \sqrt{M^2 + (2D+8)\eta^2 M + \eta^4 D^2}}{2D+2}. \tag{42}$$

D. End-to-end Tensorized Training

We provide the full description of our end-to-end tensorized training with rank determination in Alg. 1. Our key idea is to use a step of gradient-based update for the tensor factors in Φ and a step of closed-form update for the rank-control hyper parameters $\bar{\lambda}$ per iteration:

- **Step 1: Gradient Update for tensor factors:** We sample the low-rank tensor factors Φ and update all parameters of the tensor factor variational distributions using gradient descent on the loss $\mathcal{L}(q)$ of Eq. (32) with a learning rate α :

$$\Phi \leftarrow \Phi + \alpha \nabla_{\Phi} \mathcal{L}(q). \tag{43}$$

In the specific case of the CP model the gradients for the posterior variance and mean of the factor matrices are given by

$$\begin{aligned}
\nabla_{\Sigma_{ij}^{(n)}} \mathcal{L}(q) &= -z \nabla_{u_{ij}} \log p(\mathcal{D} | \{\mathbf{U}^{(n)}\}) - \frac{1}{\Sigma_{ij}^{(n)}} + \frac{\Sigma_{ij}^{(n)}}{\bar{\lambda}_j} \\
\nabla_{\overline{u_{ij}^{(n)}}} \mathcal{L}(q) &= -\nabla_{u_{ij}} \log p(\mathcal{D} | \{\mathbf{U}^{(n)}\}) + \frac{\overline{u_{ij}^{(n)}}}{\bar{\lambda}_j}.
\end{aligned} \tag{44}$$

Note that z is the random variable sampled during the forward pass due to the reparameterization in Eq. (33) and the gradients with respect the log-likelihood are computed using standard automatic differentiation. We describe the gradients for the other three tensor formats in the appendix.

- **Step 2: Incremental closed-form update for $\bar{\lambda}$:** We found empirically that incremental updates to the rank-control parameters, rather than direct assignment of the

Algorithm 1 Tensorized Training with Rank Determination

Input: Factor learning rate α , EM stepsize γ , rank cutoff ϵ , warmup epochs e_w , total epochs m , tuning epochs t

for Epoch e in $[1, \dots, m]$ **do**

Assign β according to Equation (46).

for each batch $\mathcal{B} \subset \mathcal{D}$ **do**

Update the low-rank factor distribution variational parameters as in Step 1, Equation (43).

Update the rank-control hyper-parameters as in Step 2, Equation (45).

end for

end for

Prune tensor ranks as described in Equation (48).

minimizing values $\bar{\lambda}_k^*$ from Equations (41), (42), led to better performance. Therefore we adopt an incremental update strategy with learning rate γ for the rank parameter updates:

$$\bar{\lambda}_k \leftarrow \gamma \bar{\lambda}_k^* + (1 - \gamma) \bar{\lambda}_k. \tag{45}$$

We iteratively repeat Steps 1 and 2 for a predetermined number of epochs m .

Warmup Schedule. A general challenge in Bayesian tensor computation is that poor initializations can lead to excessive rank shrinkage and trivial rank-zero solutions. In tensor completion the SVD is used to generate high-quality initializations [32], [36]. For nonlinear tensorized neural networks we randomly initialize the factor matrices so the predictive accuracy is low and the KL divergence may dominate the local loss landscape around the initialization point. To avoid trivial rank-zero local optima early in the training process we re-weight the KL divergence from the variational approximation to the prior by a factor that linearly increases from 0 to 1 during the training process. Let e_w be the number of warmup training epochs and e be the current epoch. We re-weight the KL divergence from the variational approximation to the prior by a factor β defined by

$$\beta = \min\left(1, \frac{e}{e_w}\right), \tag{46}$$

and update the loss from Eq. (32) accordingly:

$$\begin{aligned}
\mathcal{L}(q) &= -\log \mathbb{E}_{q(\{\mathbf{U}^{(n)}\}, \boldsymbol{\lambda})} p(\mathcal{D} | \{\mathbf{U}^{(n)}\}) \\
&\quad + \beta \text{KL}\left(q\left(\{\mathbf{U}^{(n)}\}, \boldsymbol{\lambda}\right) \| p\left(\{\mathbf{U}^{(n)}\}, \boldsymbol{\lambda}\right)\right).
\end{aligned} \tag{47}$$

TABLE I: Summary of different training methods.

Method	Tensorized final model	End-to-end tensorized training	Automatic rank determination
Baseline			
FR [24]	✓	✓	
TC-MR [13]	✓		
TC-OR [13]	✓		
ARD-LU (Proposed)	✓	✓	✓
ARD-HC (Proposed)	✓	✓	✓

Gradually increasing the weight of the KL divergence to the prior avoids early local optima in which all ranks shrink to zero. We have found empirically that $e_w = m/2$ is a good choice for the number of warmup steps.

Rank Pruning. After we run our Bayesian solver we truncate the ranks with variance $\bar{\lambda}_k$ below a pre-specified threshold ϵ . For example, for the CP format if $\bar{\lambda}_k < \epsilon$ we assign

$$\begin{aligned} \bar{u}_{ik}^{(n)} &\leftarrow 0 \text{ for } 1 \leq n \leq d, 1 \leq i \leq I_n, \\ \bar{\Sigma}_{ik}^{(n)} &\leftarrow 0 \text{ for } 1 \leq n \leq d, 1 \leq i \leq I_n. \end{aligned} \quad (48)$$

The associated k -th column of $\mathbf{U}^{(n)}$ is removed.

V. EXPERIMENTS

We demonstrate the applications of our tensorized end-to-end training method on several models containing fully connected layers, embedding layers and convolution layers. We also compare our method with several recent methods of tensorized neural networks by reporting the predictive accuracy on the test data set and the number of model parameters in the resulting model. Our method trains a Bayesian neural network, therefore we report the predictive accuracy of the posterior mean.

In order to evaluate and compare the performance, we implement the following methods in our experiments:

- **Baseline:** this is a standard training method, where the model parameters are neither tensorized nor compressed. We use this method as a baseline for comparison of predictive accuracy and model size.
- **TC-MR** [12], [13]: train and then compress with maximum ranks. In order to compare our method with the most popular tensorized neural network methods, we implement the method in [12], [13]. In this approach we train a non-tensorized and uncompressed neural network (equivalent to “baseline”), followed by a tensor decomposition and fine-tuning. In all experiments we fine-tune for 20 epochs. This approach requires that the user select the compression rank. Here we use the maximum rank (R for CP or $\mathbf{R} = [R_1, R_2, \dots, R_d]$ for other formats) used in our proposed Bayesian model.
- **TC-OR:** train and then compress with oracle rank (r in CP or $\mathbf{r} = [r_1, r_2, \dots, r_d]$ for other formats). This post-training compression method follows the same procedures of TC-MR [12], [13], except that it uses the “oracle rank” discovered by our proposed rank determination method. In practice the “TC-OR” method would require a combinatorial rank search over a high-dimensional

discrete space to discover the same rank as our method. Here we just assume that we know the oracle rank *a-priori* by luck in order to compare the performance of the post-training compression method with our proposed method when they have the same compressed model size.

- **FR:** Fixed-rank tensorized training. We implement the end-to-end tensorized training [24] with a tensor rank fixed *a priori*. It is hard to determine a rank properly in advance, and the model can be very inaccurate if the chosen rank parameter is too low. Therefore, we train the low-rank tensor factors with the maximum rank that is chosen for our Bayesian model in order to achieve a good accuracy.
- **ARD-LU:** this is the first version of our proposed tensorized training method with automatic rank determination. In this version, we use the log-uniform prior in (26) for the rank-control hyper-parameters. All tensor factors are initialized with a maximum rank (R for CP and $\mathbf{R} = [R, \dots, R_d]$ for other formats), and the actual ranks (r for CP and $\mathbf{r} = [r_1, \dots, r_d]$ for other formats) are automatically determined by our training process.
- **ARD-HC:** this is the second version of our proposed training method. It differs from ARD-LU only in the hyper prior: in ARD-HC we use the half-Cauchy prior (25) for the rank-control hyper parameters.

Table I has summarized the features of various methods. Clearly, our proposed methods enjoy all of the listed advantages compared with other methods. We consider four (CP, Tucker, TT and TTM) low-rank tensor formats for each tensorized method. Therefore, our experiments involve the implementation of 21 specific methods in total (20 tensorized implementations plus one baseline method).

We do not compare our method against low-rank matrix compression methods [9], [10], [11], because the previous study [24] has already shown the significantly higher compression ratios of fixed-rank tensorized training (i.e., the FR method in our experiments) than matrix compression approaches with the similar level of accuracy.

A. Synthetic Example for Rank Determination

First we test the ability of our proposed method to infer the tensor rank of model parameters in a neural network. For each tensor format we construct a synthetic version of the MNIST dataset using a one-layer tensorized neural network (equivalent to tensorized logistic regression). The tensorized layer is fully connected and the fixed tensor rank is five for each tensor format: 5 for CP, [5, 5, 5] for Tucker and [1,

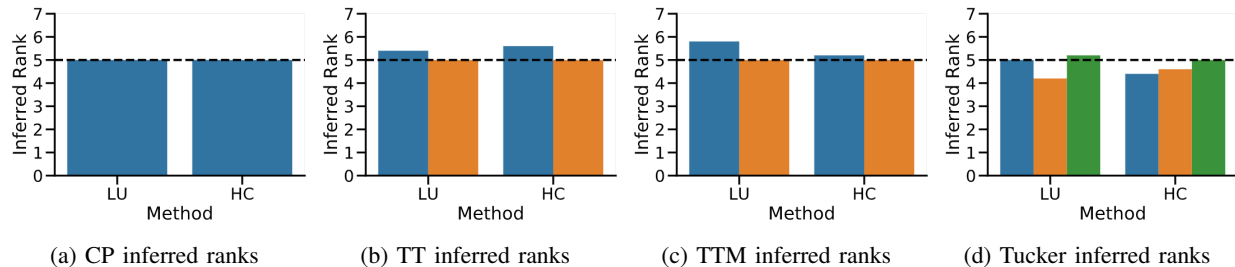


Fig. 5: The inferred ranks from a synthetic example for the rank determination task. The true rank (shown by dashed lines) equals 5 and maximum rank is set to 10. The inferred ranks of different modes are given by colored bars.

5, 5, 1] for TT/TTM. We use the rank-5 model to generate synthetic labels for the MNIST images. Then we train a set of low-rank tensorized models with a maximum rank of 10 on the synthetic dataset. For the CP, tensor-train, and Tucker formats we reshape the weight matrix $\mathbf{W} \in \mathbb{R}^{784 \times 10}$ into a tensor of shape size $[28, 28, 10]$ (i.e., an order-3 tensor of size $28 \times 28 \times 10$). For the tensor-train matrix format we use the dimensions $[4, 7, 4], [7, 2, 5]$.

We plot the mean inferred ranks for our log-uniform (LU) and half-cauchy (HC) priors in Fig. 5. We observe that our model performs well across tensor formats. The actual CP rank is exactly recovered. The inferred ranks of Tucker, TT and TTM are close to but not equal to the exact values, because tensor ranks are not unique, which is a fundamental difference between matrices and tensors.

B. MNIST

Next we apply all methods to a neural network with two fully connected layers on the MNIST dataset with images of size 28×28 . The first fully connected layer is size 784×512 and has a ReLU activation function. The second fully connected layer is size 512×10 with a softmax activation function. We list the specifications of tensorization in Table II. We use a maximum rank of 20 for all models except the CP, for which we increase the maximum rank to 50.

We observe that in all cases our automatic rank determination can achieve the highest compression ratio. Our proposed automatic rank determination both improves accuracy and reduces parameter number in all tensor formats except the TT format which has slight accuracy loss but the highest compression ratio. We hypothesize that the automatic rank reduction can reduce over-fitting on the simple MNIST task. The TTM format is best-suited to fully connected layers, achieving the second-highest compression ratios and the second-best accuracy. In Fig. 6 we plot the rank determination output of a single training run using our log-uniform prior. We note that our algorithm discovers the actual ranks that are nearly impossible to determine via hand-tuning or combinatorial search (for example $[1, 20, 3, 2, 1]$ in the TTM model from a maximum rank of $[1, 20, 20, 20, 1]$, which may require up to 16,000 searches).

C. Embedding Table for Natural Language Processing

We continue to investigate tensor approaches on a sentiment classification task from [26]. Like many NLP models, the

TABLE II: Tensorization settings for the MNIST example.

Model	Layer 1 Dimensions	Layer 2 Dimensions	Max Rank
Baseline	784×512	512×10	NA
CP	$[28, 28, 16, 32]$	$[32, 16, 10]$	50
Tucker	$[28, 28, 16, 32]$	$[32, 16, 10]$	20
TT	$[28, 28, 16, 32]$	$[32, 16, 10]$	20
TTM	$[4, 7, 4, 7], [4, 4, 8, 4]$	$[32, 16], [2, 5]$	20

TABLE III: Numerical results of the MNIST example.

Tensor Format	Model	Parameter #	Accuracy
	Baseline	407,050	98.09
CP	FR [24]	8,622 ($47.2 \times$)	97.52
	TC-MR [13]	8,622 ($47.2 \times$)	97.32
	TC-OR [13]	7,175 ($56.7 \times$)	97.36
	ARD-LU (Proposed)	7,175 ($56.7 \times$)	98.06
	ARD-HC (Proposed)	7,134 ($57.1 \times$)	97.98
Tucker	FR [24]	171,762 ($2.4 \times$)	97.93
	TC-MR [13]	171,762 ($2.4 \times$)	98.00
	TC-OR [13]	100,758 ($4.0 \times$)	97.91
	ARD-LU (Proposed)	100,758 ($4.0 \times$)	98.30
	ARD-HC (Proposed)	91,332 ($4.5 \times$)	98.30
TT	FR [24]	26,562 ($15.3 \times$)	97.78
	TC-MR [13]	26,562 ($15.3 \times$)	97.43
	TC-OR [13]	4,224 ($96.4 \times$)	96.91
	ARD-LU (Proposed)	4,224 ($96.4 \times$)	96.28
	ARD-HC (Proposed)	4,276 ($95.2 \times$)	97.04
TTM	FR [24]	29,242 ($13.9 \times$)	98.06
	TC-MR [13]	29,242 ($13.9 \times$)	97.47
	TC-OR [13]	6,144 ($66.3 \times$)	96.61
	ARD-LU (Proposed)	6,144 ($66.3 \times$)	98.24
	ARD-HC (Proposed)	5,200 ($78.3 \times$)	98.23

first layer is a large embedding table. Embedding tables are a promising target for tensor compression because their required input dimension equals the number of unique tokens in the input dataset (i.e. number of vocabulary words, number of users). Tensor compression can enforce weight sharing and dramatically reduce the parameter count of these models. Recent work in tensorized neural networks has applied the TTM format to compress large embedding tables with a high ratio [26]. We replicate a sentiment classification model on the IMDB dataset from their work. The neural network model consists of an embedding table with dimension $25,000 \times 256$, two bidirectional LSTM layers with hidden unit size 128, and a fully-connected layer with 256 hidden units. Following the benchmark model in [26] we do not tensorize these layers. Dropout masks are applied to the output of each layer except the last.

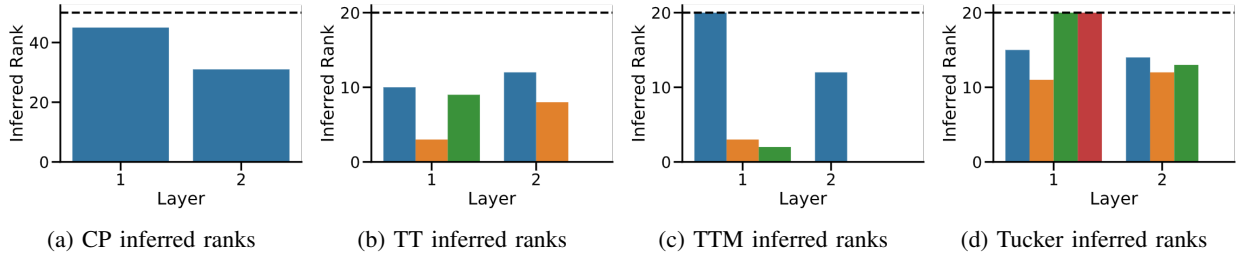


Fig. 6: Inferred ranks for one run of the MNIST experiment using a log-uniform prior. The maximum rank is given by a dashed black line. The inferred ranks are given by colored bars.

TABLE IV: Tensorization settings for the embedding table.

Model	Embedding Dimensions	Max Rank
Baseline	$25,000 \times 256$	NA
CP	[5,8,25,25,4,8,8]	50
Tucker	[25,25,40,16,16]	5
TT	[5,8,25,25,4,8,8]	20
TTM	[5,5,5,5,6,8],[2,2,2,2,4,4]	20

TABLE V: Numerical results on the embedding table.

Tensor Type	Model	Embedding Parameter #	Accuracy
	Baseline	6,400,000	88.34
CP	FR [24]	8,276 (774 \times)	87.44
	TC-MR [13]	8,276 (774 \times)	74.46
	TC-OR [13]	6,138 (1024 \times)	73.21
	ARD-LU (Proposed)	6,138 (1024 \times)	87.61
	ARD-HC (Proposed)	6,476 (998 \times)	87.54
Tucker	FR [24]	78,540 (81 \times)	87.80
	TC-MR [13]	78,540 (81 \times)	75.12
	TC-OR [13]	61,920 (103 \times)	71.97
	ARD-LU (Proposed)	61,920 (103 \times)	87.79
	ARD-HC (Proposed)	58,120 (110 \times)	88.01
TT	FR [24]	28,260 (226 \times)	85.6
	TC-MR [13]	28,260 (226 \times)	82.34
	TC-OR [13]	22,982 (278 \times)	71.81
	ARD-LU (Proposed)	22,982 (278 \times)	85.33
	ARD-HC (Proposed)	19,363 (331 \times)	85.82
TTM	FR [24]	22,312 (287 \times)	88.59
	TC-MR [13]	22,312 (287 \times)	83.79
	TC-OR [13]	15,932 (402 \times)	84.83
	ARD-LU (Proposed)	15,932 (402 \times)	88.93
	ARD-HC (Proposed)	14,275 (448 \times)	88.78

We test all four tensor formats and both tensor priors on the sentiment classification problem. The tensor dimensions and maximum ranks used to compress the embedding table are given in Table IV. We use a lower number of dimensions and a lower maximum rank for the Tucker model to avoid a large-size core tensor \mathcal{G} .

The outcomes of our experiments are reported in Table V. Compared with all other tensor approaches, our methods (ARD-LU and ARD-HC) have achieved the best compression ratio for all tensor formats at little to no accuracy cost. The TTM format outperforms all other models (including the baseline uncompressed model) in terms of accuracy, though we note that the CP model performs well despite its extremely low parameter number.

TABLE VI: Numerical results on the CNN model.

Tensor Type	Model	Parameter #	Accuracy
	Baseline	13,942,602	90.36
CP	FR [24]	652,748 (21.4 \times)	90.13
	TC-MR [13]	652,748 (21.4 \times)	75.80
	TC-OR [13]	568,412 (24.5 \times)	71.29
	ARD-LU (Proposed)	568,412 (24.5 \times)	90.18
	ARD-HC (Proposed)	593,419 (23.5 \times)	90.08
Tucker	FR [24]	653,438 (21.3 \times)	85.15
	TC-MR [13]	653,438 (21.3 \times)	85.36
	TC-OR [13]	606,201 (23.0 \times)	84.86
	ARD-LU (Proposed)	606,201 (23.0 \times)	85.41
	ARD-HC (Proposed)	589,092 (23.7 \times)	85.86
TT	FR [24]	649,328 (21.5 \times)	87.31
	TC-MR [13]	649,328 (21.5 \times)	86.02
	TC-OR [13]	376,123 (37.1 \times)	85.42
	ARD-LU (Proposed)	376,123 (37.1 \times)	86.68
	ARD-HC (Proposed)	521,096 (26.8 \times)	85.92
TTM	FR [24]	641,898 (21.7 \times)	90.04
	TC-MR [13]	641,898 (21.7 \times)	81.88
	TC-OR [13]	598,693 (22.3 \times)	80.49
	ARD-LU (Proposed)	598,693 (22.3 \times)	90.09
	ARD-HC (Proposed)	579,217 (24.1 \times)	90.02

D. CIFAR Convolutional Model

Our final test model is a convolutional neural network taken from [14]. This model consists of six convolutional layers followed by three fully connected layers. We follow [14] and tensorize all layers except the first convolution and the last fully connected layer which together contain a small fraction of the total parameters. As before, we test all four tensor formats with our rank determination approach. The results of our method, the baseline model, and the train-and-then-compress approach are reported in Table VI.

We observe that our proposed method (ARD) leads to higher accuracy than the train-and-then-compress approach. Our automatic rank determination achieves parameter reduction with only slight accuracy reduction. The CP and TTM methods outperform Tucker and TT methods for this task in terms of accuracy. Previous studies [12], [14] have shown that the compression ratio on convolution layers are often much lower than on fully connected layers due to the small size of convolution filters. Nevertheless, our tensorized training with automatic rank determination always achieves the best compression performance.

VI. CONCLUSION

This work has proposed a variational Bayesian method for the end-to-end training of tensorized neural networks. Our work has addressed the fundamental challenge of automatic rank determination, which is important for training compact neural network models on many hardware platforms (especially on resource-constraint devices). The stochastic variational inference method developed in this paper allows us to train tensorized neural networks with tens of millions of uncompressed model parameters. Our experiments have demonstrated that the proposed end-to-end tensorized training can outperform all existing tensor methods in terms of both compression ratios and prediction accuracy.

ACKNOWLEDGMENTS

We thank Kaiqi Zhang for pointing out an error in the original gradient update derivations.

APPENDIX

Tucker: In Tucker format the gradients take a similar form as in the CP format except the rank parameter is dimension-specific.

$$\begin{aligned}\nabla_{\Sigma_{ij}^{(n)}} \mathcal{L}(q) &= -z \nabla_{u_{ij}} \log p(\mathcal{D}|\mathcal{G}, \{\mathbf{U}^{(n)}\}) - \frac{1}{\Sigma_{ij}^{(n)}} + \frac{\Sigma_{ij}^{(n)}}{\lambda_j^{(n)}} \\ \nabla_{\frac{u_{ij}^{(n)}}{\lambda_j^{(n)}}} \mathcal{L}(q) &= -\nabla_{u_{ij}} \log p(\mathcal{D}|\mathcal{G}, \{\mathbf{U}^{(n)}\}) + \frac{u_{ij}^{(n)}}{\lambda_j^{(n)}}\end{aligned}\quad (49)$$

The core tensor \mathcal{G} is updated according to

$$\begin{aligned}\nabla_{\Sigma_{i_1 \dots i_d}} \mathcal{L}(q) &= -z \nabla_{\Sigma_{i_1 \dots i_d}} \log p(\mathcal{D}|\mathcal{G}, \{\mathbf{U}^{(n)}\}) - \frac{1}{\Sigma_{i_1 \dots i_d}} + \frac{\Sigma_{i_1 \dots i_d}}{\sigma_0^2} \\ \nabla_{\bar{g}_{i_1 \dots i_d}} \mathcal{L}(q) &= -\nabla_{\bar{g}_{i_1 \dots i_d}} \log p(\mathcal{D}|\mathcal{G}, \{\mathbf{U}^{(n)}\}) + \frac{\bar{g}_{i_1 \dots i_d}}{\sigma_0^2}.\end{aligned}\quad (50)$$

Tensor Train: In TT-format the parameters are re-indexed to accommodate a third dimension in addition to the dimension-specific rank parameters referenced above.

$$\begin{aligned}\nabla_{\Sigma_{ijk}^{(n)}} \mathcal{L}(q) &= -z \nabla_{g_{ijk}} \log p(\mathcal{D}|\{\mathcal{G}^{(n)}\}) - \frac{1}{\Sigma_{ijk}^{(n)}} + \frac{\Sigma_{ijk}^{(n)}}{\lambda_k^{(n)}} \\ \nabla_{\frac{g_{ijk}^{(n)}}{\lambda_k^{(n)}}} \mathcal{L}(q) &= -\nabla_{g_{ijk}} \log p(\mathcal{D}|\{\mathcal{G}^{(n)}\}) + \frac{g_{ijk}^{(n)}}{\lambda_k^{(n)}}\end{aligned}\quad (51)$$

Tensor Train Matrix: Finally, for the TTM format we perform one additional re-indexing.

$$\begin{aligned}\nabla_{\Sigma_{ijkl}^{(n)}} \mathcal{L}(q) &= -z \nabla_{g_{ijkl}} \log p(\mathcal{D}|\{\mathcal{G}^{(n)}\}) - \frac{1}{\Sigma_{ijkl}^{(n)}} + \frac{\Sigma_{ijkl}^{(n)}}{\lambda_l^{(n)}} \\ \nabla_{\frac{g_{ijkl}^{(n)}}{\lambda_l^{(n)}}} \mathcal{L}(q) &= -\nabla_{g_{ijkl}} \log p(\mathcal{D}|\{\mathcal{G}^{(n)}\}) + \frac{g_{ijkl}^{(n)}}{\lambda_l^{(n)}}\end{aligned}\quad (52)$$

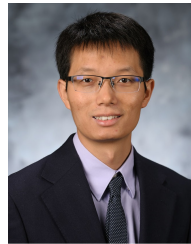
REFERENCES

- [1] K. Simonyan and A. Zisserman, "Very deep convolutional networks for large-scale image recognition," *arXiv preprint arXiv:1409.1556*, 2014.
- [2] M. Naumov, D. Mudigere, H.-J. M. Shi, J. Huang, N. Sundaraman, J. Park, X. Wang, U. Gupta, C.-J. Wu, A. G. Azzolini *et al.*, "Deep learning recommendation model for personalization and recommendation systems," *arXiv preprint arXiv:1906.00091*, 2019.
- [3] V. Sze, Y.-H. Chen, J. Emer, A. Suleiman, and Z. Zhang, "Hardware for machine learning: Challenges and opportunities," in *IEEE Custom Integrated Circuits Conference*, 2017, pp. 1–8.
- [4] J. M. Alvarez and M. Salzmann, "Compression-aware training of deep networks," in *Advances in Neural Information Processing Systems*, 2017, pp. 856–867.
- [5] S. J. Hanson and L. Y. Pratt, "Comparing biases for minimal network construction with back-propagation," in *Advances in neural information processing systems*, 1989, pp. 177–185.
- [6] Y. LeCun, J. S. Denker, and S. A. Solla, "Optimal brain damage," in *Advances in neural information processing systems*, 1990, pp. 598–605.
- [7] S. Han, H. Mao, and W. J. Dally, "Deep compression: Compressing deep neural networks with pruning, trained quantization and Huffman coding," *arXiv preprint arXiv:1510.00149*, 2015.
- [8] G. Hinton, O. Vinyals, and J. Dean, "Distilling the knowledge in a neural network," *arXiv preprint arXiv:1503.02531*, 2015.
- [9] T. N. Sainath, B. Kingsbury, V. Sindhwani, E. Arisoy, and B. Ramabhadran, "Low-rank matrix factorization for deep neural network training with high-dimensional output targets," in *Intl. Conf. Acoustics, Speech and Signal Processing*, 2013, pp. 6655–6659.
- [10] J. Xue, J. Li, and Y. Gong, "Restructuring of deep neural network acoustic models with singular value decomposition," in *Interspeech*, 2013, pp. 2365–2369.
- [11] M. Denil, B. Shakibi, L. Dinh, M. Ranzato, and N. De Freitas, "Predicting parameters in deep learning," in *Advances in neural information processing systems*, 2013, pp. 2148–2156.
- [12] Y.-D. Kim, E. Park, S. Yoo, T. Choi, L. Yang, and D. Shin, "Compression of deep convolutional neural networks for fast and low power mobile applications," *arXiv preprint arXiv:1511.06530*, 2015.
- [13] V. Lebedev, Y. Ganin, M. Rakhuba, I. Oseledets, and V. Lempitsky, "Speeding-up convolutional neural networks using fine-tuned cp-decomposition," *arXiv preprint arXiv:1412.6553*, 2014.
- [14] T. Garipov, D. Podoprikin, A. Novikov, and D. Vetrov, "Ultimate tensorization: compressing convolutional and FC layers alike," *arXiv preprint arXiv:1611.03214*, 2016.
- [15] C. Cui, C. Hawkins, and Z. Zhang, "Tensor methods for generating compact uncertainty quantification and deep learning models," in *Intl. Conf. Computer-Aided Design*, 2019, pp. 1–6.
- [16] K. Zhang, X. Zhang, and Z. Zhang, "Tucker tensor decomposition on FPGA," in *Proc. Intl. Conf. Computer-Aided Design*, 2019, pp. 1–8.
- [17] C. Deng, F. Sun, X. Qian, J. Lin, Z. Wang, and B. Yuan, "TIE: energy-efficient tensor train-based inference engine for deep neural network," in *Proceedings of the 46th International Symposium on Computer Architecture*, 2019, pp. 264–278.
- [18] S. Smith, N. Ravindran, N. D. Sidiropoulos, and G. Karypis, "Splatt: Efficient and parallel sparse tensor-matrix multiplication," in *Intl. Symp. Parallel and Distributed Processing*, 2015, pp. 61–70.
- [19] S. Smith and G. Karypis, "Tensor-matrix products with a compressed sparse tensor," in *Proceedings of the 5th Workshop on Irregular Applications: Architectures and Algorithms*, 2015, pp. 1–7.
- [20] H. Huang, L. Ni, K. Wang, Y. Wang, and H. Yu, "A highly parallel and energy efficient three-dimensional multilayer cmos-rram accelerator for tensorized neural network," *IEEE Transactions on Nanotechnology*, vol. 17, no. 4, pp. 645–656, 2017.
- [21] E. Strubell, A. Ganesh, and A. McCallum, "Energy and policy considerations for deep learning in NLP," in *Proc. Annual Meeting of the Association for Computational Linguistics*, 2019, pp. 3645–3650.
- [22] S. Teerapittayanon, B. McDanel, and H.-T. Kung, "Distributed deep neural networks over the cloud, the edge and end devices," in *Intl. Conf. Distributed Computing Systems*, 2017, pp. 328–339.
- [23] C. J. Hillar and L.-H. Lim, "Most tensor problems are NP-hard," *Journal of the ACM*, vol. 60, no. 6, p. 45, 2013.
- [24] A. Novikov, D. Podoprikin, A. Osokin, and D. P. Vetrov, "Tensorizing neural networks," in *Advances in Neural Information Processing Systems*, 2015, pp. 442–450.
- [25] G. G. Calvi, A. Moniri, M. Mahfouz, Q. Zhao, and D. P. Mandic, "Compression and interpretability of deep neural networks via tucker tensor layer: From first principles to tensor valued back-propagation," *arXiv preprint arXiv:1903.06133*, 2019.

- [26] V. Khrulkov, O. Hrinchuk, L. Mirvakhabova, and I. Oseledets, "Tensorized embedding layers for efficient model compression," *arXiv preprint arXiv:1901.10787*, 2019.
- [27] M. D. Hoffman, D. M. Blei, C. Wang, and J. Paisley, "Stochastic variational inference," *The Journal of Machine Learning Research*, vol. 14, no. 1, pp. 1303–1347, 2013.
- [28] S. Gandy, B. Recht, and I. Yamada, "Tensor completion and low-n-rank tensor recovery via convex optimization," *Inverse Problems*, vol. 27, no. 2, p. 025010, 2011.
- [29] J. Liu, P. Musialski, P. Wonka, and J. Ye, "Tensor completion for estimating missing values in visual data," *IEEE Trans. Pattern Analysis and Machine Intelligence*, vol. 35, no. 1, pp. 208–220, 2013.
- [30] D. Goldfarb and Z. Qin, "Robust low-rank tensor recovery: Models and algorithms," *SIAM Journal on Matrix Analysis and Applications*, vol. 35, no. 1, pp. 225–253, 2014.
- [31] J. A. Bazerque, G. Mateos, and G. Giannakis, "Rank regularization and bayesian inference for tensor completion and extrapolation," *IEEE Trans. Signal Processing*, vol. 61, no. 22, pp. 5689–5703, 2013.
- [32] Q. Zhao, L. Zhang, and A. Cichocki, "Bayesian CP factorization of incomplete tensors with automatic rank determination," *IEEE Trans. Pattern Analysis and Machine Intelligence*, vol. 37, no. 9, pp. 1751–1763, 2015.
- [33] H. Zhou, L. Li, and H. Zhu, "Tensor regression with applications in neuroimaging data analysis," *Journal of the American Statistical Association*, vol. 108, no. 502, pp. 540–552, 2013.
- [34] Z. Zhang, T.-W. Weng, and L. Daniel, "Big-data tensor recovery for high-dimensional uncertainty quantification of process variations," *IEEE Trans. Components, Packaging and Manufacturing Technology*, vol. 7, no. 5, pp. 687–697, 2017.
- [35] R. Guhaniyogi, S. Qamar, and D. B. Dunson, "Bayesian tensor regression," *The Journal of Machine Learning Research*, vol. 18, no. 1, pp. 2733–2763, 2017.
- [36] Q. Zhao, G. Zhou, L. Zhang, A. Cichocki, and S.-I. Amari, "Bayesian robust tensor factorization for incomplete multiway data," *IEEE transactions on neural networks and learning systems*, vol. 27, no. 4, pp. 736–748, 2016.
- [37] T. G. Kolda and B. W. Bader, "Tensor decompositions and applications," *SIAM Review*, vol. 51, no. 3, pp. 455–500, 2009.
- [38] J. D. Carroll and J.-J. Chang, "Analysis of individual differences in multidimensional scaling via an N-way generalization of "eckart-young" decomposition," *Psychometrika*, vol. 35, no. 3, pp. 283–319, 1970.
- [39] R. A. Harshman, M. E. Lundy *et al.*, "PARAFAC: Parallel factor analysis," *Computational Statistics and Data Analysis*, vol. 18, no. 1, pp. 39–72, 1994.
- [40] L. R. Tucker, "Some mathematical notes on three-mode factor analysis," *Psychometrika*, vol. 31, no. 3, pp. 279–311, 1966.
- [41] I. V. Oseledets, "Tensor-train decomposition," *SIAM Journal on Scientific Computing*, vol. 33, no. 5, pp. 2295–2317, 2011.
- [42] B. Recht, M. Fazel, and P. A. Parrilo, "Guaranteed minimum-rank solutions of linear matrix equations via nuclear norm minimization," *SIAM review*, vol. 52, no. 3, pp. 471–501, 2010.
- [43] R. M. Neal, "Bayesian learning via stochastic dynamics," in *Advances in neural information processing systems*, 1993, pp. 475–482.
- [44] —, *Bayesian learning for neural networks*. Springer Science & Business Media, 2012, vol. 118.
- [45] Q. Liu and D. Wang, "Stein variational gradient descent: A general purpose bayesian inference algorithm," in *Advances In Neural Information Processing Systems*, 2016, pp. 2378–2386.
- [46] C. Blundell, J. Cornebise, K. Kavukcuoglu, and D. Wierstra, "Weight uncertainty in neural networks," *arXiv preprint arXiv:1505.05424*, 2015.
- [47] M. I. Jordan, Z. Ghahramani, T. S. Jaakkola, and L. K. Saul, "An introduction to variational methods for graphical models," *Machine learning*, vol. 37, no. 2, pp. 183–233, 1999.
- [48] D. P. Kingma and M. Welling, "Auto-encoding variational bayes," *arXiv preprint arXiv:1312.6114*, 2013.
- [49] M. P. Wand, J. T. Ormerod, S. A. Padoan, R. Frühwirth *et al.*, "Mean field variational bayes for elaborate distributions," *Bayesian Analysis*, vol. 6, no. 4, pp. 847–900, 2011.
- [50] S. Ghosh, J. Yao, and F. Doshi-Velez, "Model selection in bayesian neural networks via horseshoe priors," *Journal of Machine Learning Research*, vol. 20, no. 182, pp. 1–46, 2019.
- [51] S. Nakajima and M. Sugiyama, "Analysis of empirical map and empirical partially bayes: Can they be alternatives to variational bayes?" in *Artificial Intelligence and Statistics*, 2014, pp. 20–28.



Cole Hawkins is a Ph.D student in the Department of Mathematics at the University of California, Santa Barbara (UCSB). He received a B.A. in mathematics from Amherst College in 2016 and an M.A. in mathematics from UCSB in 2018. His research interests include tensor computation, Bayesian inference, and uncertainty quantification.



Zheng Zhang (M'15) has been an Assistant Professor of Electrical and Computer Engineering with the University of California at Santa Barbara (UCSB), since July 2017. He received his Ph.D in Electrical Engineering and Computer Science from Massachusetts Institute of Technology (MIT), Cambridge, MA, in 2015. His research interests include uncertainty quantification and tensor computation. The applications of his research include design automation of nano-scale electronics and photonics, algorithm/hardware co-design of high-dimensional and robust/safe machine learning systems.

Dr. Zhang received three best journal paper awards from IEEE: the Best Paper Award of IEEE Transactions on Computer-Aided Design of Integrated Circuits and Systems in 2014, two Best Paper Awards of IEEE Transactions on Components, Packaging and Manufacturing Technology in 2018 and 2020, respectively. He also received two Best Paper Awards at international conferences. His PhD dissertation won the ACM SIGDA Outstanding Ph.D Dissertation Award in Electronic Design Automation in 2016, and the Best Thesis Award from the Microsystems Technology Laboratory of MIT in 2015. He received the NSF CAREER Award in 2019 and a Facebook Research Award in 2020.